REVIEW ARTICLE

Complementarity of structural biology methods: ribosome in the spotlight

Jayati Sengupta

Indian Institute of Chemical Biology, 4, Raja S.C. Mullick Road, Kolkata 700 032, India

The translational apparatus ribosome is in the limelight these days with the announcement of the 2009 Nobel Prize in Chemistry. The three winners have unveiled ribosome structures using X-ray crystallography. Ribosome 3D structures have also been studied by another emerging structural biology method named cryo-electron microscopy (cryo-EM). In the study of the structure and function of macromolecules, the 'hybrid' strategy of combining available structural data derived from various sources has been proven quite successful. This review highlights how the hybrid approach in ribosome structure analysis paves the way for a more detailed molecular understanding of the structural basis of translation.

Keywords: Crystallography, cryo-EM, hybrid-approach, ribosome, 3D-structure.

THE three Nobel laureates in chemistry for 2009, Ada Yonath of the Weizmann Institute of Science, Israel, Thomas Steitz of Yale University and Venkatraman Ramakrishnan of the Medical Research Council Laboratory of Molecular Biology in Cambridge, United Kingdom, have made groundbreaking contributions to the crystallography of ribosome, the protein factory of the cell. Decades of heroic efforts subsequently culminated in 2000 when the high-resolution crystal structures of ribosomal subunits were published independently by the groups of all three Nobel winners[1–3].

One of the most intriguing of all biological structures is the ribosome composed of ribosomal RNA and protein (ribonucleoprotein complex), responsible for translation of the genetic code to produce proteins, one of the most fundamental processes of life in all living organisms. Protein synthesis is accomplished by an interaction between the ribosome and amino-acid-bearing tRNAs, selected according to the genetic instructions of the mRNA, in the course of which the amino acids are strung together to form a polypeptide. Protein synthesis machinery is an excellent target for antibiotics. Antibiotics work by sabotaging the protein synthesis process. Better understanding of the translational apparatus allows us to design better drugs against the invading organisms[4].

e-mail: jayati@iicb.res.in

As a highly complex dynamic molecular machine, ribosome undergoes many conformational changes during the translation process due to dynamic interactions with functional ligands participating in translation. These include messenger RNA (mRNA), transfer RNA (tRNA) and many translational protein factors. Prior to the visualization of high-resolution crystal structure, the first appreciation of the structural complexity of ribosome came from another structural biology tool cryo-electron microscopy (cryo-EM) which revealed an intricate topology of the ribosome[5].

Cryo-EM offers unique opportunities because of the capability of this technique, when combined with 3D reconstruction, to directly visualize ribosomal complexes in defined functional states. The data collection of the ribosomal complexes preserved as a cryo-EM sample in the transmission electron microscope provides tens of thousands of projections showing the ribosome in random orientations. A 3D density map of the ribosomal complex can be generated using the single-particle reconstruction method. This method has made a number of significant contributions to our understanding of the translation process[6,7].

The analysis of the cryo-EM medium resolution maps on the molecular level is facilitated by the advent of high-resolution X-ray structures of ribosome, as well as by the steady improvement and progressive automation of algorithms for fitting and docking[8–11]. Clearly, far from becoming obsolete, the emergence of atomic structures by X-ray crystallography brings out the full potential of cryo-EM, and a hybrid approach, where cryo-EM and X-ray crystallography are combined together, has been proved to be useful to understand the functioning of the translational machinery[12,13].

Current status of ribosome structure determination

Ribosome crystallography

The ribosome is the largest asymmetric biological molecule, and the most complex component of a cell successfully studied via X-ray crystallography. In order to achieve the 3D structure, researchers grew crystals of ribosomes where the molecules are arranged in a regularly repeated pattern. Briefly, an intense X-ray beam

from the light source penetrates the crystal, resulting in tens of thousands of diffraction spots on a computerized imaging detector. Radiation damage can be reduced dramatically by freezing the crystals at liquid nitrogen temperature prior to data collection. Researchers measure the position and intensity of each spot, and then mathematically calculate the electron density of the sample. From these data, they are able to build a molecular model of the ribosomal structure[14,15].

Ada Yonath and co-workers reported the first 3D crystals of 50S ribosomal subunits in 1980. During the next 15 years, progress had been made only in the process of ribosome crystallization. The diffraction data collection from ribosome crystals and crystallographic computation of the data posed challenges that could not have been met in 1980s. Around 1995, improvements in areas such as detectors, synchrotron light sources, computers and crystallographic software had opened the door for solving structures of ribosomal complexity[15,16].

A profoundly challenging problem was the phasing. A decisive break through in ribosomal crystallography was when a 9 Å resolution crystallographic electron density map of the *Haloarcula marismortui* 50S subunit was published in 1998. A cryo-EM reconstruction of the ribosomal 50S subunit from Joachim Frank's group[17], along with multiple isomorphous replacement, and anomalous scattering techniques was used in phasing[18].

Many years of hard work by several X-ray crystallography groups bore fruit in 2000, and X-ray structures of the small and large ribosomal subunits of the eubacterium *Thermus thermophilus* and the archeon *H. marismortui* were published[1–3].

Functional insights from ribosome crystal structures

The magnificent structures of the two ribosomal subunits at atomic resolution have radically changed the boundary conditions of ribosome research. The wealth of information that subsequently emerged from the X-ray studies of the ribosomal subunits[1–3,19,20], complete bacterial ribosomes[21–26], as well as numerous complexes with antibiotics[4,27,28] have altered the direction and pace of research to address its unresolved issues[28–35]. It is worth mentioning that, in addition to the three Nobel awardees, Harry Noller of the University of California Santa Cruz and Peter Moore at Yale University made enormous contributions to solve the structure of the ribosome.

During the past years, remarkable developments have resulted in a much more detailed picture of ribosome dynamics. Crystallographic studies on the ligand-bound 70S ribosome molecules (see Table 1) shed light on the fundamental questions concerning the accuracy of tRNA selection during protein elongation, the tRNA translocation during elongation, and the release and recycling steps[34,36–41]. The most recent additions to this growing list are the 70S ribosome complexed with (i) elongation factor-Tu·tRNA·GDP, stabilized by the antibiotics kirromycin and paromomycin[42]; and (ii) EF-G·GDP and fusidic acid[43].

Cryo-electron microscopy of ribosome

Cryo-EM is a relatively new method of structural biology research, which – when combined with the single-particle reconstruction approach – is capable of yielding 3D density maps of macromolecules in their native, hydrated state[44]. Briefly, molecules in a buffer suspension are deposited on an electron microscope grid, and the excess liquid is blotted off so that only a thin-layer remains. The grid is then quickly plunged into liquid ethane that is kept at liquid nitrogen temperature. Under those conditions, the water turns into vitreous (amorphous) ice, without disrupting the structure of the molecule[45,46]. The use of 'low-dose imaging' ensures that the damage to the biological specimen is minimized. In the processing of the images resulting from these experiments, it is assumed that, to a first approximation, all molecules possess identical structure and that they present different orientations, covering angular space fairly uniformly. Mathematical and computational approaches have been designed to determine the orientations of the individual particles and to reconstruct the density distribution of the molecule from the projections recorded.

Application to specimens in which the macromolecule occurs in the form of isolated 'single particles' not only extends the range of specimens greatly, but also brings out the full advantage of cryo-EM: visualizing the molecule engaged in interactions with ligands[47]. Thus, in principle, all naturally occurring states have become amenable to study. In the single-particle reconstruction approach, the task of combining individual copies of a molecule into a common coordinate framework is done by the computer, using an extensive battery of mathematical procedures.

Structures of functional ribosome complexes revealed by cryo-EM

The striking similarity in overall structural features between ribosomal complexes visualized by cryo-EM and X-ray crystallography, confirms the validity of cryo-EM as a tool in structural biology (Figure 1). Despite the success in the elucidation of ribosomal structure by X-ray crystallography, the detailed mechanism by which translation of mRNA code into peptide proceeds is still not fully understood. Landmark contributions in understanding the ribosome dynamics during the four steps of translation: initiation, elongation, termination and recycling have been made by cryo-EM[48–59].

Table 1. Structures of the 70S ribosome and ribosomal subunits in complex with functional ligands solved by X-ray crystallography

No.	Factor/s bound	Species	Resolution	PDB code	Reference
1 (2001)	IF1 and the 30S ribosomal subunit	*Thermus thermophilus*	3.2 Å	1HRO	37
2 (2001)	30S + ASL of cognate tRNA (A-site) + mRNA	*Thermus thermophilus*	3.3 Å	1IBL, 1IBM	78
3 (2001)	70S + messenger RNA (mRNA) and transfer RNAs (tRNAs)	*Thermus thermophilus*	5.5 Å	1GIX, 1GIY	25
4 (2001)	70S + mRNA and tRNA	*Thermus thermophilus*	7 Å	1JGO	26
5 (2003)	70S + mRNA and tRNA	*Escherichia coli*	10 and 9 Å	1PNS, 1PNU, 1PNX, 1PNY	79
6 (2004)	50S + trigger factor	*Haloarcula marismortui*	2.7 Å	1W2B	
7 (2005)	50S + ribosome recycling factor	*Deinococcus radiodurans*	3.3 Å	1Y69	41
8 (2005)	70S + releasefactors (RF1 and RF2)	*Thermus thermophilus*	5.9 Å (RF1); 6.7 Å (RF2 complex)	2B9O, 2B9P, 2B64, 2B66, 2B9M, 2B9N	80
9 (2006)	70S + a model mRNA and two tRNAs	*Thermus thermophilus*	3.7 Å	2I1C, 1VS9	22
10 (2006)	70S + mRNA and stem loop of P-site tRNA	*Escherichia coli*	3.5 Å	2I2P, 2I2T, 2I2U, 2I2V	81
11 (2006)	70S + mRNA and tRNA	*Thermus thermophilus*	2.8 Å	2j00, 2j01, 2j02, 2j03	24
12 (2007)	70S + ribosome recycling factor and tRNA in P and E sites	*Thermus thermophilus*	3.5 Å	2V46, 2V47, 2V48, 2V49	82
13 (2008)	70S + release factor RF1, tRNA and mRNA	*Thermus thermophilus*	3.2 Å	3D5A, 3D5B, 3D5C, 3D5D	83
14 (2008)	70S + release factor RF2	*Thermus thermophilus*	3 Å	3F1E, 3F1F, 3F1G, 3F1H	38
15 (2009)	70S + anticodn stem-loop tRNA mimics	*Escherichia coli*	3.5 Å (apo) 4.0 Å (anticodon stem-loop bound)	3I1M, 3I1N, 3I1O, 3I1P, 3I1Q, 3I1R, 3I1S, 3I1T, 3I1Z, 3I20, 3I21, 3I22	84
16 (2009)	70S + EF-Tu ternary complex (with kirromycin, paromomycin)	*Thermus thermophilus*	3.6 Å	2WRN, 2WRO, 2WRQ, 2WRR	42
17 (2009)	70S + EF-G with antibiotic fusidic acid	*Thermus thermophilus*	3.6 Å	2wri, 2wrj, 2wrk, 2wrl	43
18 (2009)	70S + ribosome-dependent endonuclease RelE	*Thermus thermophilus*	3.3 Å (before) 3.6 Å (after mRNA cleavage)	3KIQ, 3KIR, 3KIS, 3KIT, 3KIU, 3KIW, 3KIX, 3KIY	85

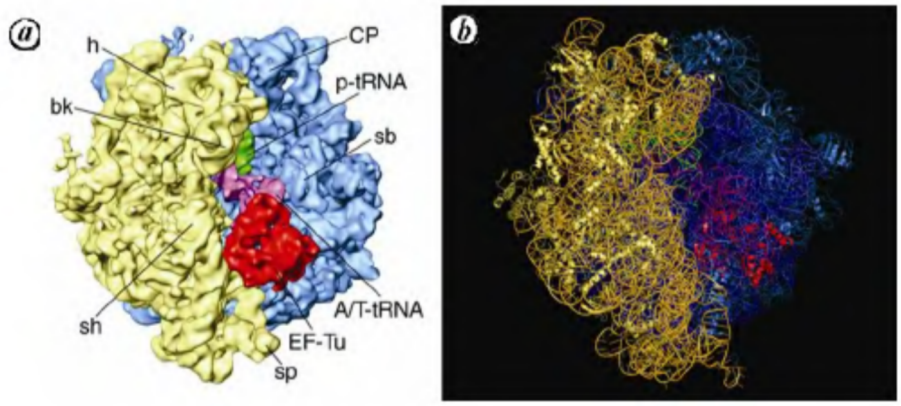

Figure 1. Resemblance of density map derived from cryo-EM with coordinates from X-ray crystallography. ***a***, 6.7 Å cryo-EM map[98] of the 70S ribosome (30S subunit: yellow; 50S subunit: blue) in complex with EF–Tu ternary complex (code EMD-5036). Landmarks in the small subunit: h, head; b, body; sh, shoulder; sp, spur; bk, beak; and in the large subunit: CP, central protuberance; sb, stalk (L7/L12 protein) base. ***b***, 70S crystal structure with the EF–Tu ternary complex[42], 16S rRNA shown in orange yellow, and small ribosomal proteins in cream yellow, 23S and 5S rRNA in dark blue, 50S ribosomal proteins in cyan blue (pdb codes 2WRN, 2WRO). In both the structures EF–Tu (red), A/T tRNA (purple), p-site tRNA (green) are shown in very similar positions.

Moreover, in gauging the role of cryo-EM in ribosome structure research, it must also be borne in mind that, despite many efforts, no atomic structure is available for a eukaryotic ribosome, and increasingly, within the past decade, cryo-EM has filled this gap[60–65]. In general, progress in structural studies of eukaryotic ribosomes has

Table 2. Cryo-EM maps depicting eukaryotic ribosomes and ribosomal complexes

Category	Ribosome	No.	Species	Complex with	Reference
Cytoplasmic ribosome		1	*Saccharomyces cerevisiae*	p-site tRNA,	63
				eEF2,	64
				channel complexes,	60
				cricket paralysis virus (CrPV) IRES-bound	86
	Fungal 80S				
		2	*Thermomyces lanuginosus*	eEF2	87
	Algal 80S	1	*Chlamydomonas reinhardtii* (green alga)	empty	88
	Protozoan 80S	1	*Trypanosoma cruzi*	empty	89
	Plant 80S	1	Wheat germ	Signal recognition particle (SRP)-bound	62
		1	Rat (liver)	empty	90
		2	Rabbit (reticulocyte)	empty	91
	Animal 80S	3	Canine (microsomal membranes)	empty,	92
				channel complexes	61, 93
		4	Human (*HeLa* cells)	CrPV IRES-bound	94
Organellar ribosome		1	*Leishmania tarentolae*		95
	Mitochondrial ribosome	2	*Bos taurus*		96
	Chloroplast ribosome	1	Spinach		97

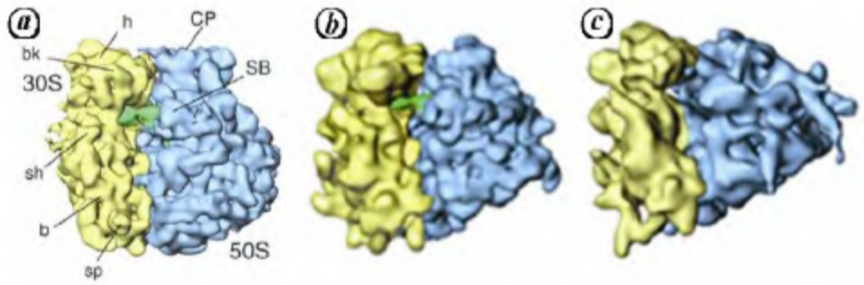

Figure 2. Comparison of the architecture of ribosomes from different species solved by cryo-EM and single particle reconstruction technique. ***a***, 11.5 Å *E. coli* 70S ribosome (ref. 99, code EMD-1003); ***b***, 15.4 Å yeast 80S ribosome (ref. 63, code EMD-1076); ***c***, 18.3 Å human ribosome (ref. 94, code EMD-1093). All three maps are viewed from the intersubunit factor-binding side. Landmarks in panel ***a*** are defined as in Figure 1.

lagged behind that of prokaryotes. Nevertheless, significant advances have been made in the past couple of years. The structures of eukaryotic ribosomes and ribosomal functional complexes (see Table 2) from various species have been visualized at medium resolution via cryo-EM in conjunction with single particle reconstruction technique. The architecture of the intersubunit space of ribosomes from prokaryotes and eukaryotes is fundamentally the same and appears to have been highly conserved during the process of evolution. On the outer surface, however, eukaryotic ribosomes show more complex, extended structures, which reflect the larger size of the rRNAs and the greater number of ribosomal proteins present in these ribosomes (Figure 2).

A hybrid approach

A cryo-EM reconstruction can be interpreted at a level of detail that is greater than the experimental resolution if high-resolution structures of components are available. This is because an atomic model can be placed into a moderate-resolution cryo-EM reconstruction using constrained fitting, with an improved accuracy of placement over the experimental resolution of the cryo-EM map[66,67]. The density map generated by the cryo-EM represents the Coulomb potential distribution of the object and can thus be readily and quantitatively compared with the electron density maps obtained by X-ray crystallography, providing the basis for molecular docking. To some extent, the pieces of structural information provided by these two methods complement each other, helping to bridge the resolution gap.

In the past few years, computational methods have been developed to make this initial fitting more objective (automated) and quantitative, and to go beyond the mere rigid fitting of atomic structures, taking into account conformational changes by flexible fitting as well. It is this 'hybrid' approach that has resulted in the rapid proliferation of cryo-EM as a technique for investigating

Figure 3. Comparison of the atomic structures of EF–Tu·tRNA·GDP ternary complex from cryo-EM fitting and X-ray crystallography structures. ***a***, Crystal structure of isolated EF–Tu ternary complex (pdb code 1OB2). ***b***, Model of the ternary complex fitted into the EF–Tu ternary complex density visualized in the cryo-EM map of the ternary complex-bound 70S ribosome complex[49]. ***c***, Crystal structure of the EF–Tu ternary complex bound to the 70S ribosome[42]. Both ***b*** and ***c*** show the 'bent' conformation of the anticodon stem loop (ASL). Figures were rendered using PyMol.

macromolecular structure and dynamics. In the following, we will discuss some of the methods of fitting and docking.

For fitting atomic models into cryo-EM maps, either one of two routes can be taken: (i) interactive manual fitting or (ii) computerized, automated fitting. Until recently, manual fitting has been the method of choice. Several graphics programs (e.g. O: (http://xray.bmc.uu.se/~alwyn/); Quanta: Accelrys, Inc., San Diego, USA; PyMol (http://pymol.sourceforge.net/)) that contain an interactive user interface are available.

An example is the discovery of twisted tRNA intermediate conformation during codon recognition process[68]. Manual fitting of the tRNA crystal structure, considering each loop as a rigid-body, resulted in a meaningful interpretation of the tRNA mass observed in the cryo-EM map[49,69]. The overall shape of the fitted molecule shows a bent conformation at the anticodon loop of the tRNA that allows the molecule to reach the decoding centre, and that explains several findings deduced from previous biochemical experiments. The 'bent' conformation of the tRNA molecule was supported by a recent crystal structure[42] of EF-Tu ternary complex-bound 70S ribosome depicting the intricate details of the EF-Tu-ribosome interactions (Figure 3).

A variety of rigid-body docking programmes have been developed to facilitate automated fitting of the lower-resolution EM density maps (Autodock (http://autodock.scripps.edu/), EMFIT (http://bilbo.bio.purdue.edu/~viruswww/Rossmann_home/softwares/emfit.php)). Moreover, flexible fitting approaches to fit multiple, interconnected components are also used in several methods described here.

Flexible fitting approach

To state the flexible fitting approach in a general way, each domain of a multi-domain protein can be treated, in approximation, as a rigid body (unless the crystal structure proves the existence of strong interactions among some domains) that are able to move with respect to one another within certain constraints. This piece-wise flexible fitting approach has obvious potential in the interpretation of cryo-EM maps depicting ribosome in two different functional states.

This approach is implemented in a programme called RsRef (real-space refinement technique[10]) to achieve multiple-domain fitting in a quantitative way where following a least-squares optimization, the positions of the structural elements are refined, and, at the same time, stereo-chemical conflicts are minimized. This method was successfully used to obtain quasi-atomic models for two cryo-EM density maps, separated by large conformational changes, depicting the ribosome in two phases of translocation[70,71]. The results provided molecular interpretation of the conformational changes of the subunits during 'ratchet-like rotation', previously identified by visual analysis, where the small subunit rotates relative to the large subunit[72].

Flexible fitting based on normal modes and molecular dynamics simulations

Real-space refinement, even though following a quantitative protocol, still cannot do justice to the intricacies of conformational changes, since the 'rigid body' approach is an approximation. There are two other approaches to the problem of flexible fitting that both attempt to predict the conformational mobility based on the knowledge of the atomic structure: fitting based on normal modes, and fitting based on molecular dynamics simulations.

Normal mode analysis (NMA), when applied to the X-ray structures of macromolecular assemblies, has been able to predict large interdomain motions deduced from cryo-EM experiments[73]. NMA uses a simplified elastic network representation, where the mechanical system is modelled as a network of mass points connected with springs that represent inter-residue interactions[11]. Normal mode-based flexible fitting (NMFF) has been success-

fully applied to elucidate the structural basis of protein translocation through the protein-conducting channel (PCC) bound to the ribosome[74].

The time-dependent behaviour of a molecule is more closely and more realistically captured by molecular dynamics (MD) simulations. The molecular dynamics flexible fitting (MDFF) method incorporates the EM data as an external potential added to the molecular dynamics force field, allowing all internal features present in the EM map to be used in the fitting process, while the model remains fully flexible and stereochemically correct[75]. In a recent study, MDFF method was applied to obtain an atomic model of a 6.7 Å cryo-EM map of the 70S ribosome bound to the EF–Tu·tRNA·GDP ternary complex stalled by the antibiotic kirromycin that enabled the interpretation of the cryo-EM data in unprecedented detail[76].

Conclusion

Although achieving the ultimate goal of atomic resolution using single particle, cryo-EM is still a challenging task (particularly for asymmetric molecules like ribosome), cryo-EM is becoming increasingly mature, with the proliferation of computational resources and methodological advancement. Meanwhile, a hybrid approach, where the medium resolution cryo-EM map is interpreted by fitting the atomic structures of identifiable components, has become a powerful tool. To this end, several computer-assisted or entirely automated flexible fitting techniques have been developed within the past decade. X-ray structures for the ribosomal subunits and the 70S ribosomes have profoundly changed our knowledge base, and given cause for a reflection on the future role cryo-EM can play in the study of structure and function of the ribosome.

In contrast to NMR and X-ray techniques, cryo-EM is yet to be developed in India. On the other hand, several groups in India study macromolecules ranging from 500 kDa to few MDa which are ideally suited for structural studies using cryo-EM and 3D reconstruction techniques. Encouraging fact is that a low resolution cryo-EM structure (~20–22 Å) of *Vibrio cholerae* haemolysin oligomer, the first cryo-EM study from India, has been reported this year[77].

1. Ban, N., Nissen, P., Hansen, J., Moore, P. B. and Steitz, T. A., The complete atomic structure of the large ribosomal subunit at 2.4 Å resolution. *Science*, 2000, **289**, 905–920.
2. Schluenzen, F. *et al.*, Structure of functionally activated small ribosomal subunit at 3.3 angstroms resolution. *Cell*, 2000, **102**, 615–623.
3. Wimberly, B. T. *et al.*, Structure of the 30S ribosomal subunit. *Nature*, 2000, **407**, 327–339.
4. Wimberly, B. T., The use of ribosomal crystal structures in antibiotic drug design. *Curr. Opin. Investig. Drugs*, 2009, **10**, 750–765.
5. Frank, J., The ribosome at higher resolution – the donut takes shape. *Curr. Opin. Struct. Biol.*, 1997, **7**, 266–272.
6. Frank, J., Toward an understanding of the structural basis of translation. *Genome Biol.*, 2003, **4**, 237.
7. van Heel, M., Unveiling ribosomal structures: the final phases. *Curr. Opin. Struct. Biol.*, 2000, **10**, 259–264.
8. Rossmann, M. G., Bernal, R. and Pletnev, S. V., Combining electron microscopic with X-ray crystallographic structures. *J. Struct. Biol.*, 2001, **136**, 190–200.
9. Topf, M., Lasker, K., Webb, B., Wolfson, H., Chiu, W. and Sali, A., Protein structure fitting and refinement guided by cryo-EM density. *Structure*, 2008, **16**, 295–307.
10. Fabiola, F. and Chapman, M. S., Fitting of high-resolution structures into electron microscopy reconstruction images. *Structure*, 2005, **13**, 389–400.
11. Tama, F. and Brooks, C. L., Symmetry, form, and shape: guiding principles for robustness in macromolecular machines. *Annu. Rev. Biophys. Biomol. Struct.*, 2006, **35**, 115–133.
12. Mitra, K. and Frank, J., Ribosome dynamics: insights from atomic structure modeling into cryo-electron microscopy maps. *Annu. Rev. Biophys. Biomol. Struct.*, 2006, **35**, 299–317.
13. Russell, R. B. *et al.*, A structural perspective on protein–protein interactions. *Curr. Opin. Struct. Biol.*, 2004, **14**, 313–324.
14. Moore, P. B., The ribosome at atomic resolution. *Biochemistry*, 2001, **40**, 3243–3250.
15. Yonath, A., The search and its outcome: high-resolution structures of ribosomal particles from mesophilic, thermophilic, and halophilic bacteria at various functional states. *Annu. Rev. Biophys. Biomol. Struct.*, 2002, **31**, 257–273.
16. Ramakrishnan, V. and Moore, P. B., Atomic structures at last: the ribosome in 2000. *Curr. Opin. Struct. Biol.*, 2001, **11**, 144–154.
17. Penczek, P., Ban, N., Grassucci, R. A., Agrawal, R. K. and Frank, J., Haloarcula marismortui 50S subunit-complementarity of electron microscopy and X-ray crystallographic information. *J. Struct. Biol.*, 1999, **128**, 44–50.
18. Moore, P. B. and Steitz, T. A., The ribosome revealed. *Trends Biochem. Sci.*, 2005, **30**, 281–283.
19. Harms, J. *et al.*, High resolution structure of the large ribosomal subunit from a mesophilic eubacterium. *Cell*, 2001, **107**, 679–688.
20. Ogle, J. M., Brodersen, D. E., Clemons Jr, W. M., Tarry, M. J., Carter, A. P. and Ramakrishnan, V., Recognition of cognate transfer RNA by the 30S ribosomal subunit. *Science*, 2001, **292**, 897–902.
21. Dunham, C. M., Selmer, M., Phelps, S. S., Kelley, A. C., Suzuki, T., Joseph, S. and Ramakrishnan, V., Structures of tRNAs with an expanded anticodon loop in the decoding center of the 30S ribosomal subunit. *Rna*, 2007, **13**, 817–823.
22. Korostelev, A., Trakhanov, S., Laurberg, M. and Noller, H. F., Crystal structure of a 70S ribosome-tRNA complex reveals functional interactions and rearrangements. *Cell*, 2006, **126**, 1065–1077.
23. Schuwirth, B. S., Borovinskaya, M. A., Hau, C. W., Zhang, W., Vila-Sanjurjo, A., Holton, J. M. and Cate, J. H., Structures of the bacterial ribosome at 3.5 Å resolution. *Science*, 2005, **310**, 827–834.
24. Selmer, M. *et al.*, Structure of the 70S ribosome complexed with mRNA and tRNA. *Science*, 2006, **313**, 1935–1942.
25. Yusupov, M. M., Yusupova, G. Z., Baucom, A., Lieberman, K., Earnest, T. N., Cate, J. H. and Noller, H. F., Crystal structure of the ribosome at 5.5 Å resolution. *Science*, 2001, **292**, 883–896.
26. Yusupova, G. Z., Yusupov, M. M., Cate, J. H. and Noller, H. F., The path of messenger RNA through the ribosome. *Cell*, 2001, **106**, 233–241.
27. Schlunzen, F., Harms, J. M., Franceschi, F., Hansen, H. A., Bartels, H., Zarivach, R. and Yonath, A., Structural basis for the

antibiotic activity of ketolides and azalides. *Structure*, 2003, **11**, 329–338.
28. Yonath, A., High-resolution structures of large ribosomal subunits from mesophilic eubacteria and halophilic archaea at various functional states. *Curr. Protein Pept. Sci.*, 2002, **3**, 67–78.
29. Moore, P. B., Structural biology. A ribosomal coup: *E. coli* at last! *Science*, 2005, **310**, 793–795.
30. Moore, P. B. and Steitz, T. A., The structural basis of large ribosomal subunit function. *Annu. Rev. Biochem.*, 2003, **72**, 813–850.
31. Noller, H. F., RNA structure: reading the ribosome. *Science*, 2005, **309**, 1508–1514.
32. Ogle, J. M., Carter, A. P. and Ramakrishnan, V., Insights into the decoding mechanism from recent ribosome structures. *Trends Biochem. Sci.*, 2003, **28**, 259–266.
33. Ramakrishnan, V., Ribosome structure and the mechanism of translation. *Cell*, 2002, **108**, 557–572.
34. Ramakrishnan, V., What we have learned from ribosome structures. *Biochem. Soc. Trans.*, 2008, **36**, 567–574.
35. Schmeing, T. M. and Ramakrishnan, V., What recent ribosome structures have revealed about the mechanism of translation. *Nature*, 2009, **461**, 1234–1242.
36. Borovinskaya, M. A. *et al.*, Structural basis for aminoglycoside inhibition of bacterial ribosome recycling. *Nat. Struct. Mol. Biol.*, 2007, **14**, 727–732.
37. Carter, A. P., Clemons Jr, W. M., Brodersen, D. E., Morgan-Warren, R. J., Hartsch, T., Wimberly, B. T. and Ramakrishnan, V., Crystal structure of an initiation factor bound to the 30S ribosomal subunit. *Science*, 2001, **291**, 498–501.
38. Korostelev, A. *et al.*, Crystal structure of a translation termination complex formed with release factor RF2. *Proc. Natl. Acad. Sci. USA*, 2008, **105**, 19684–19689.
39. Weixlbaumer, A., Jin, H., Neubauer, C., Voorhees, R. M., Petry, S., Kelley, A. C. and Ramakrishnan, V., Insights into translational termination from the structure of RF2 bound to the ribosome. *Science*, 2008, **322**, 953–956.
40. Petry, S., Weixlbaumer, A. and Ramakrishnan, V., The termination of translation. *Curr. Opin. Struct. Biol.*, 2008, **18**, 70–77.
41. Wilson, D. N. *et al.*, X-ray crystallography study on ribosome recycling: the mechanism of binding and action of RRF on the 50S ribosomal subunit. *EMBO J.*, 2005, **24**, 251–260.
42. Schmeing, T. M., Voorhees, R. M., Kelley, A. C., Gao, Y. G., Murphy, F. V. T., Weir, J. R. and Ramakrishnan, V., The crystal structure of the ribosome bound to EF–Tu and aminoacyl-tRNA. *Science*, 2009, **326**, 688–694.
43. Gao, Y. G., Selmer, M., Dunham, C. M., Weixlbaumer, A., Kelley, A. C. and Ramakrishnan, V., The structure of the ribosome with elongation factor G trapped in the posttranslocational state. *Science*, 2009, **326**, 694–699.
44. Frank, J., Single-particle reconstruction of biological macromolecules in electron microscopy – 30 years. *Q. Rev. Biophys.*, 2009, **42**, 139–158.
45. Grassucci, R. A., Taylor, D. J. and Frank, J., Preparation of macromolecular complexes for cryo-electron microscopy. *Nat. Protoc.*, 2007, **2**, 3239–3246.
46. Grassucci, R. A., Taylor, D. and Frank, J., Visualization of macromolecular complexes using cryo-electron microscopy with FEI Tecnai transmission electron microscopes. *Nat. Protoc.*, 2008, **3**, 330–339.
47. Saibil, H. R., Macromolecular structure determination by cryo-electron microscopy. *Acta Crystallogr. D Biol. Crystallogr.*, 2000, **56**, 1215–1222.
48. Rawat, U. B. *et al.*, A cryo-electron microscopic study of ribosome-bound termination factor RF2. *Nature*, 2003, **421**, 87–90.
49. Valle, M. *et al.*, Incorporation of aminoacyl-tRNA into the ribosome as seen by cryo-electron microscopy. *Nat. Struct. Biol.*, 2003, **10**, 899–906.
50. Valle, M., Zavialov, A., Sengupta, J., Rawat, U., Ehrenberg, M. and Frank, J., Locking and unlocking of ribosomal motions. *Cell*, 2003, **114**, 123–134.
51. Agrawal, R. K. *et al.*, Visualization of ribosome-recycling factor on the *Escherichia coli* 70S ribosome: functional implications. *Proc. Natl. Acad. Sci. USA*, 2004, **101**, 8900–8905.
52. Connell, S. R. *et al.*, Structural basis for interaction of the ribosome with the switch regions of GTP-bound elongation factors. *Mol. Cell*, 2007, **25**, 751–764.
53. Connell, S. R. *et al.*, A new tRNA intermediate revealed on the ribosome during EF4-mediated back-translocation. *Nat. Struct. Mol. Biol.*, 2008, **15**, 910–915.
54. Frank, J., Gao, H., Sengupta, J., Gao, N. and Taylor, D. J., The process of mRNA–tRNA translocation. *Proc. Natl. Acad. Sci. USA*, 2007, **104**, 19671–19678.
55. Frank, J., Sengupta, J., Gao, H., Li, W., Valle, M., Zavialov, A. and Ehrenberg, M., The role of tRNA as a molecular spring in decoding, accommodation and peptidyl transfer. *FEBS Lett.*, 2005, **579**, 959–962.
56. Agrawal, R. K., Penczek, P., Grassucci, R. A. and Frank, J., Visualization of elongation factor G on the *Escherichia coli* 70S ribosome: the mechanism of translocation. *Proc. Natl. Acad. Sci. USA*, 1998, **95**, 6134–6138.
57. Stark, H. *et al.*, Arrangement of tRNAs in pre- and posttranslocational ribosomes revealed by electron cryomicroscopy. *Cell*, 1997, **88**, 19–28.
58. Stark, H., Rodnina, M. V., Rinke-Appel, J., Brimacombe, R., Wintermeyer, W. and van Heel, M., Visualization of elongation factor Tu on the *Escherichia coli* ribosome. *Nature*, 1997, **389**, 403–406.
59. Stark, H., Rodnina, M. V., Wieden, H. J., van Heel, M. and Wintermeyer, W., Large-scale movement of elongation factor G and extensive conformational change of the ribosome during translocation. *Cell*, 2000, **100**, 301–309.
60. Beckmann, R. *et al.*, Architecture of the protein-conducting channel associated with the translating 80S ribosome. *Cell*, 2001, **107**, 361–372.
61. Chandramouli, P. *et al.*, Structure of the mammalian 80S ribosome at 8.7 Å resolution. *Structure*, 2008, **16**, 535–548.
62. Halic, M., Becker, T., Pool, M. R., Spahn, C. M., Grassucci, R. A., Frank, J. and Beckmann, R., Structure of the signal recognition particle interacting with the elongation-arrested ribosome. *Nature*, 2004, **427**, 808–814.
63. Spahn, C. M., Beckmann, R., Eswar, N., Penczek, P. A., Sali, A., Blobel, G. and Frank, J., Structure of the 80S ribosome from *Saccharomyces cerevisiae* – tRNA–ribosome and subunit–subunit interactions. *Cell*, 2001, **107**, 373–386.
64. Spahn, C. M. *et al.*, Domain movements of elongation factor eEF2 and the eukaryotic 80S ribosome facilitate tRNA translocation. *EMBO J.*, 2004, **23**, 1008–1019.
65. Andersen, C. B. *et al.*, Structure of eEF3 and the mechanism of transfer RNA release from the E-site. *Nature*, 2006, **443**, 663–668.
66. Chiu, W., Baker, M. L. and Almo, S. C., Structural biology of cellular machines. *Trends Cell Biol.*, 2006, **16**, 144–150.
67. Rossmann, M. G., Fitting atomic models into electron-microscopy maps. *Acta Crystallogr. D Biol. Crystallogr.*, 2000, **56**, 1341–1349.
68. Yarus, M., Valle, M. and Frank, J., A twisted tRNA intermediate sets the threshold for decoding. *RNA*, 2003, **9**, 384–385.
69. Valle, M. *et al.*, Cryo-EM reveals an active role for aminoacyl-tRNA in the accommodation process. *EMBO J.*, 2002, **21**, 3557–3567.
70. Gao, H. *et al.*, Study of the structural dynamics of the *E. coli* 70S ribosome using real-space refinement. *Cell*, 2003, **113**, 789–801.
71. Gao, H. and Frank, J., Molding atomic structures into intermediate-resolution cryo-EM density maps of ribosomal complexes using real-space refinement. *Structure*, 2005, **13**, 401–406.

72. Frank, J. and Agrawal, R. K., A ratchet-like inter-subunit reorganization of the ribosome during translocation. *Nature*, 2000, **406**, 318–322.
73. Tama, F., Valle, M., Frank, J. and Brooks (3rd), C. L., Dynamic reorganization of the functionally active ribosome explored by normal mode analysis and cryo-electron microscopy. *Proc. Natl. Acad. Sci. USA*, 2003, **100**, 9319–9323.
74. Mitra, K. *et al.*, Structure of the *E. coli* protein-conducting channel bound to a translating ribosome. *Nature*, 2005, **438**, 318–324.
75. Trabuco, L. G., Villa, E., Mitra, K., Frank, J. and Schulten, K., Flexible fitting of atomic structures into electron microscopy maps using molecular dynamics. *Structure*, 2008, **16**, 673–683.
76. Villa, E. *et al.*, Ribosome-induced changes in elongation factor Tu conformation control GTP hydrolysis. *Proc. Natl. Acad. Sci. USA*, 2009, **106**, 1063–1068.
77. Dutta, S., Mazumdar, B., Banerjee, K. K. and Ghosh, A. N., Three-dimensional structure of different functional forms of the Vibrio cholerae hemolysin oligomer: a cryo-electron microscopic study. *J. Bacteriol.*, 2010, **192**, 169–178.
78. Ferbitz, L., Maier, T., Patzelt, H., Bukau, B., Deuerling, E. and Ban, N., Trigger factor in complex with the ribosome forms a molecular cradle for nascent proteins. *Nature*, 2004, **431**, 590–596.
79. Vila-Sanjurjo, A., Ridgeway, W. K., Seymaner, V., Zhang, W., Santoso, S., Yu, K. and Cate, J. H., X-ray crystal structures of the WT and a hyper-accurate ribosome from *Escherichia coli*. *Proc. Natl. Acad. Sci. USA*, 2003, **100**, 8682–8687.
80. Petry, S. *et al.*, Crystal structures of the ribosome in complex with release factors RF1 and RF2 bound to a cognate stop codon. *Cell*, 2005, **123**, 1255–1266.
81. Berk, V., Zhang, W., Pai, R. D. and Cate, J. H., Structural basis for mRNA and tRNA positioning on the ribosome. *Proc. Natl. Acad. Sci. USA*, 2006, **103**, 15830–15834.
82. Weixlbaumer, A., Petry, S., Dunham, C. M., Selmer, M., Kelley, A. C. and Ramakrishnan, V., Crystal structure of the ribosome recycling factor bound to the ribosome. *Natl. Struct. Mol. Biol.*, 2007, **14**, 733–737.
83. Laurberg, M., Asahara, H., Korostelev, A., Zhu, J., Trakhanov, S. and Noller, H. F., Structural basis for translation termination on the 70S ribosome. *Nature*, 2008, **454**, 852–857.
84. Zhang, W., Dunkle, J. A. and Cate, J. H., Structures of the ribosome in intermediate states of ratcheting. *Science*, 2009, **325**, 1014–1017.
85. Neubauer, C. *et al.*, The structural basis for mRNA recognition and cleavage by the ribosome-dependent endonuclease RelE. *Cell*, 2009, **139**, 1084–1095.
86. Schuler, M. *et al.*, Structure of the ribosome-bound cricket paralysis virus IRES RNA. *Nat. Struct. Mol. Biol.*, 2006, **13**, 1092–1096.
87. Taylor, D. J., Nilsson, J., Merrill, A. R., Andersen, G. R., Nissen, P. and Frank, J., Structures of modified eEF2 80S ribosome complexes reveal the role of GTP hydrolysis in translocation. *EMBO J.*, 2007, **26**, 2421–2431.
88. Manuell, A. L., Yamaguchi, K., Haynes, P. A., Milligan, R. A. and Mayfield, S. P., Composition and structure of the 80S ribosome from the green alga *Chlamydomonas reinhardtii*: 80S ribosomes are conserved in plants and animals. *J. Mol. Biol.*, 2005, **351**, 266–279.
89. Gao, H., Ayub, M. J., Levin, M. J. and Frank, J., The structure of the 80S ribosome from Trypanosoma cruzi reveals unique rRNA components. *Proc. Natl. Acad. Sci. USA*, 2005, **102**, 10206–10211.
90. Dube, P. *et al.*, The 80S rat liver ribosome at 25 Å resolution by electron cryomicroscopy and angular reconstitution. *Structure*, 1998, **6**, 389–399.
91. Dube, P., Bacher, G., Stark, H., Mueller, F., Zemlin, F., van Heel, M. and Brimacombe, R., Correlation of the expansion segments in mammalian rRNA with the fine structure of the 80S ribosome; a cryoelectron microscopic reconstruction of the rabbit reticulocyte ribosome at 21 Å resolution. *J. Mol. Biol.*, 1998, **279**, 403–421.
92. Morgan, D. G., Menetret, J. F., Neuhof, A., Rapoport, T. A. and Akey, C. W., Structure of the mammalian ribosome-channel complex at 17 Å resolution. *J. Mol. Biol.*, 2002, **324**, 871–886.
93. Menetret, J. F., Hegde, R. S., Aguiar, M., Gygi, S. P., Park, E., Rapoport, T. A. and Akey, C. W., Single copies of Sec61 and TRAP associate with a nontranslating mammalian ribosome. *Structure*, 2008, **16**, 1126–1137.
94. Spahn, C. M., Jan, E., Mulder, A., Grassucci, R. A., Sarnow, P. and Frank, J., Cryo-EM visualization of a viral internal ribosome entry site bound to human ribosomes: the IRES functions as an RNA-based translation factor. *Cell*, 2004, **118**, 465–475.
95. Sharma, M. R., Booth, T. M., Simpson, L., Maslov, D. A. and Agrawal, R. K., Structure of a mitochondrial ribosome with minimal RNA. *Proc. Natl. Acad. Sci. USA*, 2009, **106**, 9637–9642.
96. Sharma, M. R., Koc, E. C., Datta, P. P., Booth, T. M., Spremulli, L. L. and Agrawal, R. K., Structure of the mammalian mitochondrial ribosome reveals an expanded functional role for its component proteins. *Cell*, 2003, **115**, 97–108.
97. Sharma, M. R., Wilson, D. N., Datta, P. P., Barat, C., Schluenzen, F., Fucini, P. and Agrawal, R. K., Cryo-EM study of the spinach chloroplast ribosome reveals the structural and functional roles of plastid-specific ribosomal proteins. *Proc. Natl. Acad. Sci. USA*, 2007, **104**, 19315–19320.
98. LeBarron, J., Grassucci, R. A., Shaikh, T. R., Baxter, W. T., Sengupta, J. and Frank, J., Exploration of parameters in cryo-EM leading to an improved density map of the *E. coli* ribosome. *J. Struct. Biol.*, 2008, **164**, 24–32.
99. Gabashvili, I. S., Agrawal, R. K., Spahn, C. M., Grassucci, R. A., Svergun, D. I., Frank, J. and Penczek, P., Solution structure of the *E. coli* 70S ribosome at 11.5 Å resolution. *Cell*, 2000, **100**, 537–549.

ACKNOWLEDGEMENTS. I thank Manidip Shasmal, and Biprashekhar Chakraborty for assistance with the preparation of figures and tables. The financial assistance from the Indian Institute of Chemical Biology, Kolkata, India and the Council of Scientific and Industrial Research, Govt of India, is gratefully acknowledged.

Received 9 December 2009; revised accepted 19 May 2010